Organic Electronics 23 (2015) 105–109

Contents lists available at ScienceDirect

Organic Electronics

journal homepage: www.elsevier.com/locate/orgel

Utilising solution processed zirconium acetylacetonate as an electron extracting layer in both regular and inverted small molecule organic photovoltaic cells

I. Hancox *, E. New, T.S. Jones

Department of Chemistry, University of Warwick, Coventry, CV4 7AL, UK

ARTICLE INFO

Article history:
Received 19 January 2015
Received in revised form 30 March 2015
Accepted 19 April 2015
Available online 20 April 2015

Keywords:
Organic solar
Buffer layer
Electron extracting layer
ZrAcac
Phthalocyanine
OPV

ABSTRACT

Interfacial layers are commonly employed in organic photovoltaic (OPV) cells in order to improve device performance. These layers must be transparent, stable, be compatible with the photo-active materials and provide efficient charge extraction with a good energetic match to the relevant organic material. In this report we demonstrate the compatibility of zirconium acetylacetonate (ZrAcac) electron extracting layers in both regular and inverted small molecule OPV cells. When the ZrAcac was processed in both air and under N_2, low work function (3.9 and 3.7 eV respectively), highly transparent layers were formed, with good energetic alignment to both C_{60} and hexachlorinated boron subphthalocyanine chloride (Cl_6-SubPc) acceptors. Initial measurements indicate similar stabilities when using the ZrAcac in either device architecture. These results indicate that the ZrAcac layer can be used as a direct replacement for the commonly used bathocuproine (BCP) in small molecule OPV cells.

1. Introduction

Organic photovoltaic (OPV) cells show great promise as a source of cheap and flexible renewable energy [1]. In recent years the performance of laboratory scale OPV cells have begun to reach the efficiencies required to consider commercialisation [2]. The incremental improvements in cell performance have been achieved through the use of new photo-active materials, cell architectures and electrodes [3–9]. However, in order to achieve the optimum cell performance for a specific photo-active system a judicious choice of the interfacial hole and electron extracting layers is also required [10,11]. The desired polarity of the cell, method and conditions of fabrication, photo-active material class and properties, and the electrodes all impact on the choice of interfacial layer. In some cases, the method of interfacial layer preparation will dictate the elected cell polarity. The requirement of high temperature annealing for some electron extracting layers is one such example, forcing the use of inverted cells to avoid damaging the organic layers [12]. Thus, a wide choice of interfacial layers are necessary to allow OPV manufacturers to match the properties required for the specific photo-active materials used in OPV cells.

A number of electron extracting materials have been employed in both polymer and small molecule based OPV cells. Reese et al. showed that low work function metals such as Ca and Ba provided a suitable contact in bulk heterojunction polymer OPV cells [13]. However, the stability of these materials is an issue. Another group of electron extracting materials are low work function metal oxides, such as TiO_x and ZnO [14,15], which have both been used in standard and inverted polymer cell architectures [14,16–18]. ZnO layers have shown versatility through fabrication using a variety of methods, including solution processing, electro-deposition and pulsed laser deposition (PLD) [18–21]. Despite this, small molecule OPV cells typically incorporate the organic material bathocuproine (BCP) as the electron extracting layer [22,23]. Rand et al. demonstrated that charge transport though BCP was facilitated by defect states within the BCP band gap, induced by hot metal penetration during deposition [22]. This indicates that BCP is only suitable for use in regular architecture small molecule cells. This limitation was confirmed by Hao et al., who reported that BCP required doping with Ag in order to obtain efficient inverted small molecule devices [24]. Additionally, BCP is also known to crystallise over time [25]. Consequently, alternative more compatible materials would be desirable for the small molecule OPV cell community.

Recently, Tan et al. utilised a zirconium acetylacetonate (ZrAcac) layer as an electron extracting layer in regular architecture polymer: fullerene bulk heterojunction OPV cells [26]. Since the layer required no subsequent processing steps and used very

* Corresponding author.
E-mail address: i.hancox@warwick.ac.uk (I. Hancox).

http://dx.doi.org/10.1016/j.orgel.2015.04.019
1566-1199/

small concentrations of ZrAcac, it showed great promise for use in flexible large area polymer OPV cells. Whilst the ZrAcac layer provided efficient electron extraction for regular architecture bulk heterojunction polymer cells, the compatibility of the layer with small molecule systems, in both regular and inverted architectures, requires testing to further understand the potential widespread applications of the layer. A direct comparison of ZrAcac processed in air and under N_2 would also be beneficial, since other solution processed interfacial layers have shown that preparation conditions can significantly influence cell performance [27,28].

In this report, ZrAcac is found to be compatible for use in both regular and inverted architecture small molecule OPV cells. The ZrAcac film provides similar cell performance when spin coated from a very low concentration solution processed in air ($ZrAcac_{air}$) or under N_2 ($ZrAcac_{N2}$), indicating the versatility of the film. In each case a highly transparent, low work function layer is produced. The inverted and regular architecture cells achieve similar cell stabilities when testing under constant illumination in air. The results demonstrate that ZrAcac is an attractive alternative to the commonly used BCP in small molecule OPV cells.

2. Experimental

ZrAcac films were fabricated by making solutions of 1 mg ml^{-1} of zirconium (IV) acetylacetonate (98%, Sigma Aldrich) in isopropanol under either a N_2 atmosphere or in air, followed by spin coating at 2000 rpm. All cells were fabricated on indium tin oxide (ITO) covered glass substrates (15 Ω sq^{-1}, Thin Film Devices) in either regular or inverted architectures. All other layers were deposited using a Kurt J. Lesker Spectros system with a base pressure of 1×10^{-8} mbar. C_{60} (Nano-C Inc, 99.5%) was purified by vacuum gradient sublimation prior to deposition, whilst boron subphthalocyanine chloride (SubPc, Lumtec, 99%) and molybdenum oxide (MoO_x, Aldrich, 99.99%) were used as received. The Al cathode was deposited *in situ* through a shadow mask, giving devices with an active area of 0.16 cm^2.

The current–voltage (J–V) characteristics of the OPV cells were measured under simulated AM1.5G solar illumination at 100 mW cm^{-2} from a Newport Oriel solar simulator using a Keithley 2400 sourcemeter for current detection. The light intensity was measured using a Fraunhofer calibrated silicon photodiode (PV Measurements Inc).

UV/vis electronic absorption spectra were obtained using a Perkin-Elmer Lambda 25 spectrometer. Atomic force microscopy (AFM) images were obtained from an Asylum Research MFP-3D (Santa Barbara, USA) in AC mode, using AC240TS cantilevers. Kelvin probe (KP) measurements were used to determine the surface work function, under a N_2 atmosphere with a reference of freshly cleaved highly ordered pyrolytic graphite (HOPG). Photoluminescence measurements were taken using a Horiba FluoroLog-3 spectrofluorometer with excitation at 580 nm.

3. Results and discussion

There are several key characteristics to consider when selecting a viable electron extracting layer. The film must be highly transparent across the wavelengths that the photo-active material absorb, have a surface free of defects and pin holes, and possess a favourable energetic alignment for electron extraction from the lowest unoccupied molecular orbital (LUMO) of the organic acceptor [10,11]. Therefore, these properties were explored in the characterisation of the ZrAcac layers, before incorporation into small molecule OPV cells.

The transmittance spectra of bare ITO, ITO/$ZrAcac_{air}$ and ITO/$ZrAcac_{N2}$ are displayed in Fig. 1. Both methods of preparing the

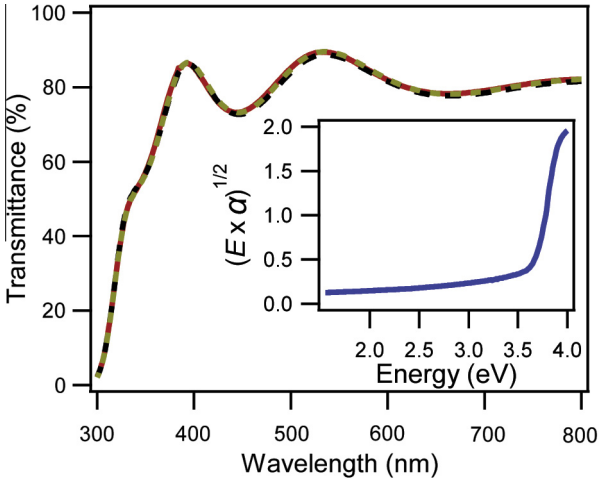

Fig. 1. Transmittance of bare ITO (gold dashed), ITO/$ZrAcac_{air}$ (black dashed) and ITO/$ZrAcac_{N2}$ (red solid). Inset: plot of $(E \times \alpha)^{1/2}$ against energy for a $ZrAcac_{air}$ layer formed on quartz using a concentrated solution (10 mg ml^{-1}), taken against a quartz background. (For interpretation of the references to colour in this figure legend, the reader is referred to the web version of this article.)

interfacial layers produce highly transparent films, with only very small losses in comparison to bare ITO. The inset of Fig. 1 shows a plot of $(E \times \alpha)^{1/2}$ against energy for a $ZrAcac_{air}$ layer made from a higher concentration of ZrAcac (10 mg ml^{-1}) on quartz, where E is energy in eV and α is absorbance. From this plot the band gap of $ZrAcac_{air}$ is shown to be very wide at 3.7 eV, and is the reason for the high transparency of the spin coated films between 300 and 800 nm.

The surface morphology of electron extracting layers can have a significant influence on cell performance. Since a small molecule donor/acceptor system with a total thickness of either 30 nm or 54 nm was to be fabricated onto the ZrAcac layers, smooth and homogeneous surface topographies are required so as not to create pin holes or large protruding features. The surface topographies of ITO, ITO/$ZrAcac_{air}$ and ITO/$ZrAcac_{N2}$ were obtained using an AFM in

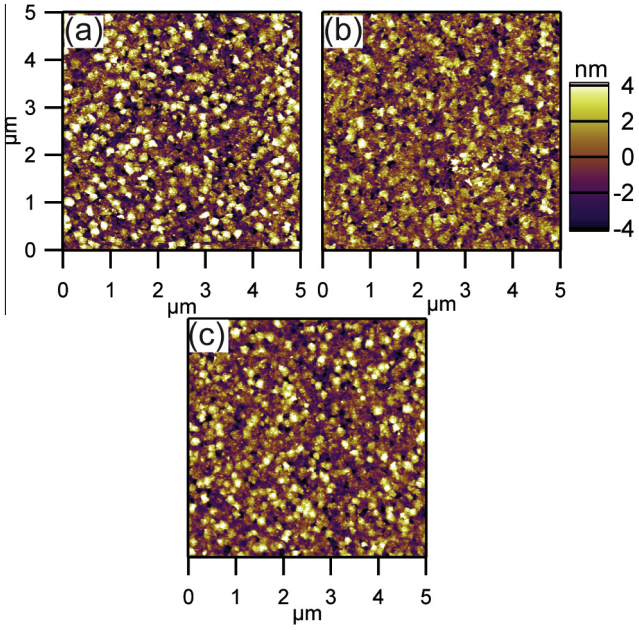

Fig. 2. 5 μm AFM topographical images of (a) bare ITO, (b) ITO/$ZrAcac_{air}$ and (c) ITO/$ZrAcac_{N2}$. All images have the same height scale (±4.05 nm).

AC mode, displayed in Fig. 2. The surface roughness (R_q) values were 2.5 nm, 2.0 nm and 2.0 nm for ITO, ITO/ZrAcac$_{air}$ and ITO/ZrAcac$_{N2}$ respectively. These smooth films, with similar surface features, provide a good interface for subsequent organic growth and device fabrication. Additionally, step edge AFM measurements indicate that the ZrAcac layer prepared in this manner has a thickness of between 1 and 2 nm.

In order to maximise the built-in field (V_{bi}) of an OPV cell and to minimise losses in the open-circuit voltage (V_{oc}), the interfacial contacts either side of the photo-active materials must have favourable energetic alignment to the relevant organic semiconductor. In the case of electron extracting materials this requires a low work function contact. Since the electron affinity of C_{60} has been shown to be 4.4 to 4.5 eV [29,30], this indicates the work function of the electron extracting material ideally should be close to or lower than 4.4 eV [31,32]. Furthermore, for hexachlorinated boron subphthalocyanine chloride (Cl_6-SubPc) an electron affinity of 3.7 eV has been reported and so a contact with a very low work function is required [33,34]. Therefore, the work functions of ITO, ITO/ZrAcac$_{air}$ and ITO/ZrAcac$_{N2}$ were measured using the KP technique. This measurement demonstrated work functions of 4.5 eV, 3.9 eV and 3.7 eV for ITO, ITO/ZrAcac$_{air}$ and ITO/ZrAcac$_{N2}$ respectively. The low work function values measured for both methods of ZrAcac layer fabrication indicate a good contact with the C_{60} and Cl_6-SubPc acceptors in OPV cells is possible.

Photoluminescence (PL) measurements were carried out in order to determine whether the ZrAcac layer is exciton blocking or only hole blocking. For direct comparisons, 15 nm layers of the Cl_6-SubPc acceptor material were deposited onto quartz (reference measurement), quartz/ZrAcac and quartz/BCP. The PL measurements obtained are shown in Fig. 3. The data shows that the ZrAcac quenches 92% of the peak emission at 630 nm, whereas BCP quenches marginally less, with 85% at 630 nm. These measurements indicate that the ZrAcac layer acts only as a hole blocking layer and not as an exciton blocking layer. This may lead to a small loss in cell performance, however the quenching shown here is only marginally greater than that of BCP.

Regular and inverted small molecule cells were fabricated using the ZrAcac electron extracting layers. The inverted cells comprised

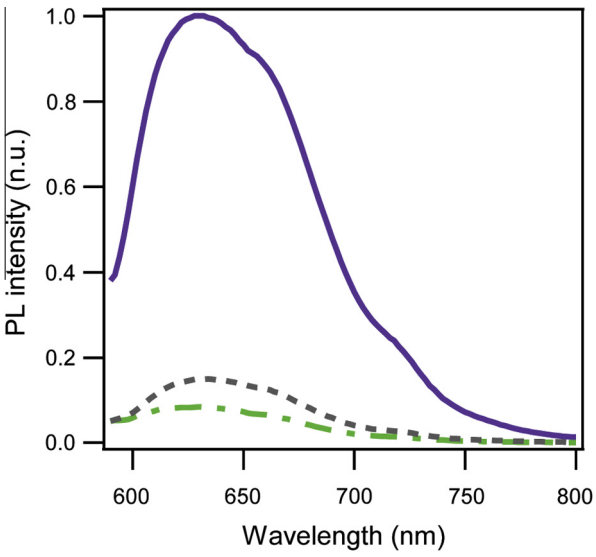

Fig. 3. PL emission spectra for 15 nm of Cl_6-SubPc on quartz (purple solid line), quartz/ZrAcac (green dot dashed line) and quartz/BCP (grey dashed line), at an excitation wavelength of 580 nm. (For interpretation of the references to colour in this figure legend, the reader is referred to the web version of this article.)

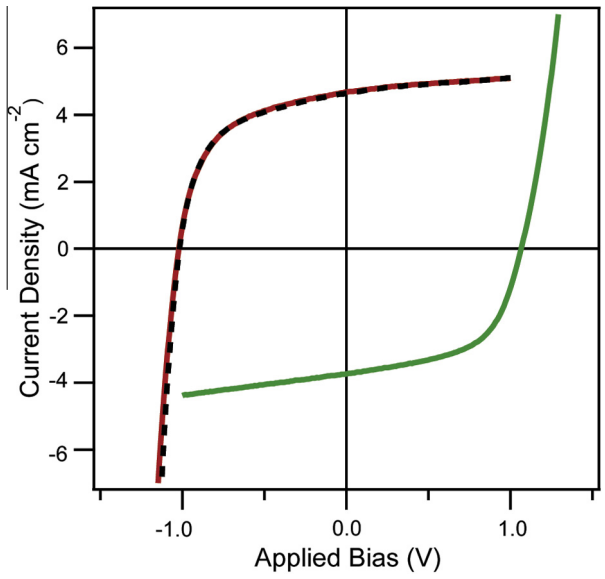

Fig. 4. *J–V* curves obtained under 1 sun illumination for inverted cells with the architecture: ITO/ZrAcac (air or N_2)/40 nm C_{60}/14 nm SubPc/10 nm MoO_x/Al, where ZrAcac$_{air}$ (black dashed) and ZrAcac$_{N2}$ (red solid). A regular architecture cell (green solid) is also shown, with the architecture ITO/5 nm MoO_x/14 nm SubPc/40 nm C_{60}/ZrAcac$_{N2}$/Al. (For interpretation of the references to colour in this figure legend, the reader is referred to the web version of this article.)

of ITO/ZrAcac$_{(air/N2)}$/40 nm C_{60}/14 nm SubPc/10 nm MoO_x/Al. The *J–V* characteristic plots are shown in Fig. 4. Inverted cells fabricated on both ZrAcac$_{air}$ and ZrAcac$_{N2}$ were deposited simultaneously to avoid batch-to-batch variation due to minor changes to the properties of the photo-active materials (such as material purity). The *J–V* curves in Fig. 4 indicate that efficient electron extraction is achieved using both ZrAcac$_{air}$ and ZrAcac$_{N2}$ layers, with no kinks present that would be indicative of barriers to charge extraction. Cells on ZrAcac$_{air}$ achieve a short circuit current density (J_{sc}) of 4.66 mA cm^{-2}, a V_{oc} of 1.02 V, a fill factor (*FF*) of 0.55 and an overall power conversion efficiency (η_p) of 2.61%. The cells fabricated on ZrAcac$_{N2}$ achieve a J_{sc} of 4.57 mA cm^{-2}, a V_{oc} of 1.02 V, a *FF* of 0.56 and a η_p of 2.60%. Therefore, values for all key cell parameters are nearly identical for both methods of film preparation and comparable to the same photoactive system deposited in inverted cells on other efficient electron extracting layers [12,35]. This comparison shows that the atmospheric conditions of ZrAcac preparation can be chosen to best match the conditions of fabrication for the photo-active layers.

The effect of depositing the ZrAcac$_{N2}$ layers on top of the organic photo-active materials was tested in regular architecture cells, with *J–V* curves shown in Fig. 4. These cells have the architecture ITO/5 nm MoO_x/14 nm SubPc/40 nm C_{60}/ZrAcAc$_{N2}$/Al and were fabricated in separate growths to the inverted cells. These cells produced a J_{sc} of 3.74 mA cm^{-2}, a V_{oc} of 1.07 V, a *FF* of 0.56 and η_p of 2.22%. The higher V_{oc} and lower J_{sc} values obtained for the SubPc/C_{60} system in regular architectures compared to inverted cells were also demonstrated in similar cell architectures by Morris and Shtein [35].

The regular architecture cell results also indicate efficient electron extraction and that the spin coated solution does not damage the thermally evaporated photo-active layers due to lack of solubility of the photo-active materials in isopropanol. Since the ZrAcac layers presented in this work do not require post deposition thermal annealing and use isopropanol as the solvent, they are very versatile for use with a number of photo-active systems in both regular and inverted architectures and could also be incorporated within tandem OPV cells.

In order to test if the ZrAcac electron extracting layers were compatible with other small molecule acceptor systems, cells replacing C_{60} with Cl_6-SubPc were fabricated. Since Cl_6-SubPc has a small electron affinity of 3.7 eV, it achieves high V_{oc} values when used in combination with the SubPc donor material [33]. Regular cells with the architecture ITO/5 nm MoO_x/15 nm SubPc/20 nm Cl_6-SubPc/$ZrAcac_{N2}$ or 8 nm BCP/Al were tested, with the *J–V* characteristics plots displayed in Fig. 5. When using the $ZrAcac_{N2}$ layer on top of the photoactive materials the cells produced a J_{sc} of 3.06 mA cm^{-2}, a V_{oc} of 1.32 V, a *FF* of 0.58 and η_p of 2.31%. The reference cell containing BCP achieved a J_{sc} of 3.10 mA cm^{-2}, a V_{oc} of 1.33 V, a *FF* of 0.59 and η_p of 2.39%. This indicates that the ZrAcac layer is compatible with other electron accepting small molecules, even with small electron affinity values, achieving a comparable performance to the reference cell fabricated simultaneously.

Cells using the SubPc/Cl_6-SubPc photoactive system were also fabricated in an inverted architecture: ITO/$ZrAcac_{N2}$ or 8 nm BCP/15 nm Cl_6-SubPc/15 nm SubPc/40 nm MoO_x/Al. The *J–V* characteristics plots for these cells are displayed in Fig. 6. Here, a 40 nm layer of MoO_x was used as an optical spacer layer to maximise current generation in these cells [19]. When utilising the $ZrAcac_{N2}$ layer the cells produced a J_{sc} of 3.59 mA cm^{-2}, a V_{oc} of 1.34 V, a *FF* of 0.53 and η_p of 2.54%. However, when using BCP as the electron extracting layer the cells produced a J_{sc} of 3.62 mA cm^{-2}, a V_{oc} of 1.29 V, a *FF* of 0.47 and η_p of 2.20%. Whilst the J_{sc} obtained with both electron transport layers is similar, there is a small loss in V_{oc} when using BCP and an even greater loss in *FF*. This is also demonstrated by the clear increase in series resistance that causes the kink in the *J–V* plot for the cells using BCP, shown in Fig. 6. Without the defect states induced by the penetration of hot aluminium that occurs in regular architecture cells, the BCP layer provides poorer initial cell performance in comparison to ZrAcac [22–24].

Whilst high initial cell performances are vital in measuring the potential of an OPV cell architecture, the stability of the cells is also an important criterion when considering materials for future technologies. Here, both the inverted and regular architecture cells using the ZrAcac electron extracting layer were tested over 1 h of constant illumination at 100 mW cm^{-2} in air. The most significant loss of performance will occur during in the first hour of illumination within the 'burn-in period', due to the photo-active materials [36,37]. Reports have shown that OPV cell performance degrades linearly after the burn-in period [36]. However, if a significant proportion of the cell performance is lost during this initial period then the cells are of little use for development. Fig. 7 displays the stability measurement of key cell parameters for regular and inverted cells containing the ZrAcac electron extracting layer. Each architecture retained ~85% of the original η_p. Both architectures also give similar losses in J_{sc}, V_{oc} and *FF*. Regular architecture cells retained *FF* marginally better, whereas inverted cells retained

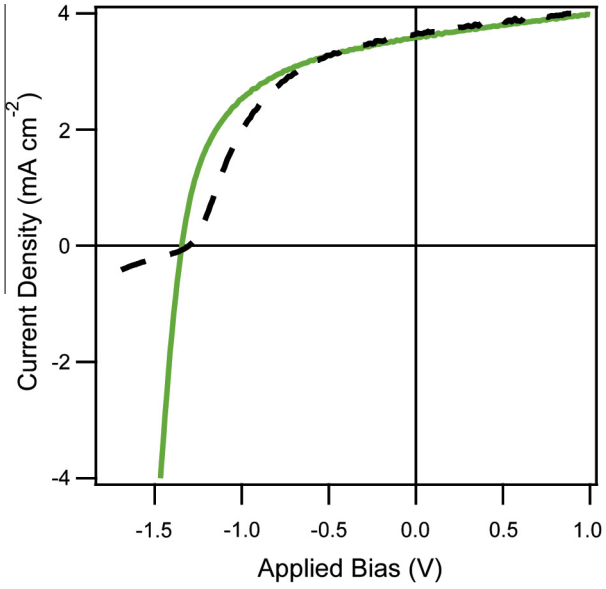

Fig. 6. *J–V* curves obtained under 1 sun illumination for inverted cells with the architecture: ITO/$ZrAcac_{N2}$ (green solid line) or BCP (black dashed line)/15 nm Cl_6-SubPc/15 nm SubPc/40 nm MoO_x/Al. (For interpretation of the references to colour in this figure legend, the reader is referred to the web version of this article.)

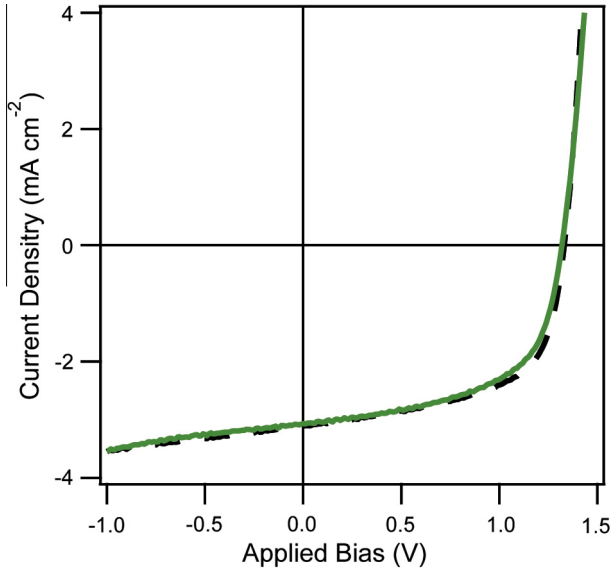

Fig. 5. *J–V* curves obtained under 1 sun illumination for inverted cells with the architecture: ITO/5 nm MoO_x/15 nm SubPc/20 nm Cl_6-SubPc/$ZrAcac_{N2}$ (green solid line) or BCP (black dashed line)/Al. (For interpretation of the references to colour in this figure legend, the reader is referred to the web version of this article.)

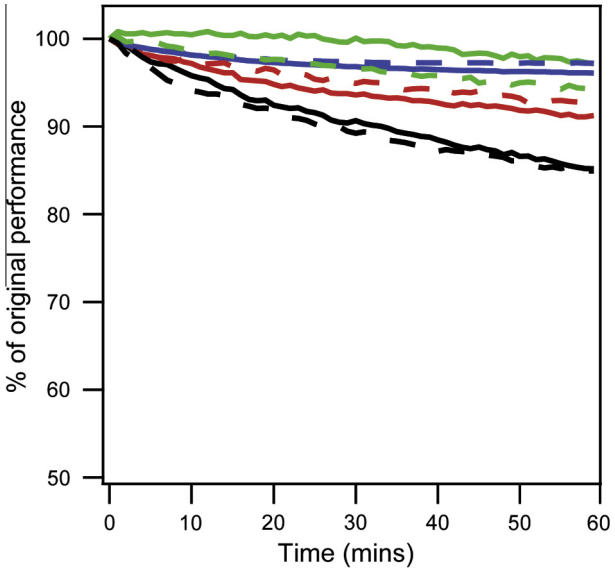

Fig. 7. Stability measurements of regular (solid) and inverted (dashed) SubPc/C_{60} cells containing ZrAcac electron transporting layers performed in air under 60 min of constant illumination at 1 sun. Key cell parameters η_p (black), J_{sc} (red), V_{oc} (blue) and *FF* (green) shown. (For interpretation of the references to colour in this figure legend, the reader is referred to the web version of this article.)

J_{sc} and V_{oc} slightly better over the hour. The results are comparable to other SubPc/C_{60} architectures utilising BCP [28,33,38]. The results indicate that the ZrAcac layers are not the limiting factor in the initial cell stability testing period. The measurements also indicate that spin coating a solution processed interfacial layer on top of the thermally evaporated acceptor surface does not impact either initial or short term cell performance. Further long term stability measurements would be worthy of future investigation, but are beyond the scope of this report.

4. Conclusions

In summary, layers of ZrAcac fabricated in both air and under N_2 have provided efficient electron extraction for inverted small molecule OPV cells using both C_{60} and Cl_6-SubPc accepting materials. The layer provided similar performance for regular architecture small molecule OPV cells for both systems, without damaging the performance of the discrete C_{60} or Cl_6-SubPc acceptor layers. For inverted SubPc/Cl_6-SubPc cells the ZrAcac layer gave preferential performance compared to BCP. For regular SubPc/Cl_6-SubPc cells the ZrAcac layer achieved a comparable performance to that of BCP, which is commonly employed in this architecture. The ZrAcac layers fabricated under both conditions preparation conditions were found to be low work function, allowing an energetic match to a wide range of acceptor materials. The ZrAcac was found to dissociate excitons from PL measurements and so acts as only a hole blocking layer. Initial stability measurements indicate that both cell architectures give a similar stability, further highlighting the potential to use ZrAcac in either architecture. The results presented here indicate the potential of using the inexpensive, low concentration, solution processed ZrAcac electron extracting layer with small molecule OPV cells. The ZrAcac layers are a viable alternative to BCP, commonly employed within regular architecture small molecule cells, whilst also allowing the fabrication of efficient inverted cells.

Acknowledgements

I. Hancox and E. New are supported by the TSB/EPSRC project "Development of Prototype High Efficiency Multi-Junction Organic Solar Cells (#100900 and EP/J500057/1).

References

[1] N. Espinosa, M. Hosel, D. Angmo, F.C. Krebs, Energy Environ. Sci. 5 (1) (2012) 5117–5132.
[2] C.C. Chen, W.H. Chang, K. Yoshimura, K. Ohya, J.B. You, J. Gao, Z.R. Hong, Y. Yang, Adv. Mater. 26 (32) (2014) 5670.
[3] G.E. Morse, J.L. Gantz, K.X. Steirer, N.R. Armstrong, T.P. Bender, ACS Appl. Mater. Interfaces 6 (3) (2014) 1515–1524.
[4] G.E. Morse, T.P. Bender, ACS Appl. Mater. Interfaces 4 (10) (2012) 5055–5068.
[5] Y.Y. Liang, Z. Xu, J.B. Xia, S.T. Tsai, Y. Wu, G. Li, C. Ray, L.P. Yu, Adv. Mater. 22 (20) (2010) E135.
[6] S. Wakim, S. Beaupre, N. Blouin, B.R. Aich, S. Rodman, R. Gaudiana, Y. Tao, M. Leclerc, J. Mater. Chem. 19 (30) (2009) 5351–5358.
[7] F. Guo, X.D. Zhu, K. Forberich, J. Krantz, T. Stubhan, M. Salinas, M. Halik, S. Spallek, B. Butz, E. Spiecker, T. Ameri, N. Li, P. Kubis, D.M. Guldi, G.J. Matt, C.J. Brabec, Adv. Energy Mater. 3 (8) (2013) 1062–1067.
[8] T.C. Hauger, S.M.I. Al-Rafia, J.M. Buriak, ACS Appl. Mater. Interfaces 5 (23) (2013) 12663–12671.
[9] N.K. Unsworth, I. Hancox, C.A. Dearden, P. Sullivan, M. Walker, R.S. Lilley, J. Sharp, T.S. Jones, Org. Electron. 15 (10) (2014) 2624–2631.
[10] E.L. Ratcliff, B. Zacher, N.R. Armstrong, J. Phys. Chem. Lett. 2 (11) (2011) 1337–1350.
[11] R. Po, C. Carbonera, A. Bernardi, N. Camaioni, Energy Environ. Sci. 4 (2) (2011) 285–310.
[12] E. New, I. Hancox, L.A. Rochford, M. Walker, C.A. Dearden, C.F. McConville, T.S. Jones, J. Mater. Chem. A 2 (45) (2014) 19201–19207.
[13] M.O. Reese, M.S. White, G. Rumbles, D.S. Ginley, S.E. Shaheen, Appl. Phys. Lett. 92 (5) (2008) 053307.
[14] J.Y. Kim, S.H. Kim, H.H. Lee, K. Lee, W.L. Ma, X. Gong, A.J. Heeger, Adv. Mater. 18 (5) (2006) 572–576.
[15] J.-C. Wang, W.-T. Weng, M.-Y. Tsai, M.-K. Lee, S.-F. Horng, T.-P. Perng, C.-C. Kei, C.-C. Yu, H.-F. Meng, J. Mater. Chem. 20 (5) (2010) 862–866.
[16] S. Schumann, R. Da Campo, B. Illy, A.C. Cruickshank, M.A. McLachlan, M.P. Ryan, D.J. Riley, D.W. McComb, T.S. Jones, J. Mater. Chem. 21 (7) (2011) 2381–2386.
[17] H. Kim, J.H. Seo, S. Cho, Appl. Phys. Lett. 99 (21) (2011) 213302.
[18] A.K.K. Kyaw, D.H. Wang, D. Wynands, J. Zhang, T.Q. Nguyen, G.C. Bazan, A.J. Heeger, Nano Lett. 13 (8) (2013) 3796–3801.
[19] C.A. Dearden, M. Walker, N. Beaumont, I. Hancox, N.K. Unsworth, P. Sullivan, C.F. McConville, T.S. Jones, Phys. Chem. Chem. Phys. 16 (35) (2014) 18926–18932.
[20] A.C. Cruickshank, S.E.R. Tay, B.N. Illy, R. Da Campo, S. Schumann, T.S. Jones, S. Heutz, M.A. McLachlan, D.W. McComb, D.J. Riley, M.P. Ryan, Chem. Mater. 23 (17) (2011) 3863–3870.
[21] J.B. Franklin, J.B. Gilchrist, J.M. Downing, K.A. Roy, M.A. McLachlan, J. Mater. Chem. C 2 (1) (2014) 84–89.
[22] B.P. Rand, J. Li, J.G. Xue, R.J. Holmes, M.E. Thompson, S.R. Forrest, Adv. Mater. 17 (22) (2005) 2714.
[23] H. Gommans, B. Verreet, B.P. Rand, R. Muller, J. Poortmans, P. Heremans, J. Genoe, Adv. Funct. Mater. 18 (22) (2008) 3686–3691.
[24] X. Hao, S.H. Wang, W. Fu, T. Sakurai, S. Masuda, K. Akimoto, Org. Electron. 15 (8) (2014) 1773–1779.
[25] Q.L. Song, F.Y. Li, H. Yang, H.R. Wu, X.Z. Wang, W. Zhou, J.M. Zhao, X.M. Ding, C.H. Huang, X.Y. Hou, Chem. Phys. Lett. 416 (1–3) (2005) 42–46.
[26] Z.A. Tan, S.S. Li, F.Z. Wang, D.P. Qian, J. Lin, J.H. Hou, Y.F. Li, Sci. Rep. 4 (2014) 9.
[27] E.L. Ratcliff, J. Meyer, K.X. Steirer, A. Garcia, J.J. Berry, D.S. Ginley, D.C. Olson, A. Kahn, N.R. Armstrong, Chem. Mater. 23 (22) (2011) 4988–5000.
[28] I. Hancox, L.A. Rochford, D. Clare, M. Walker, J.J. Mudd, P. Sullivan, S. Schumann, C.F. McConville, T.S. Jones, J. Phys. Chem. C 117 (1) (2013) 49–57.
[29] S.W. Cho, L.F.J. Piper, A. DeMasi, A.R.H. Preston, K.E. Smith, K.V. Chauhan, P. Sullivan, R.A. Hatton, T.S. Jones, J. Phys. Chem. C 114 (4) (2010) 1928–1933.
[30] Y. Kim, M. Shin, I. Lee, H. Kim, S. Heutz, Appl. Phys. Lett. 92 (9) (2008) 093306.
[31] A. Crispin, X. Crispin, M. Fahlman, M. Berggren, W.R. Salaneck, Appl. Phys. Lett. 89 (21) (2006) 213503.
[32] S. Braun, W.R. Salaneck, M. Fahlman, Adv. Mater. 21 (14–15) (2009) 1450–1472.
[33] P. Sullivan, A. Duraud, I. Hancox, N. Beaumont, G. Mirri, J.H.R. Tucker, R.A. Hatton, M. Shipman, T.S. Jones, Adv. Energy Mater. 1 (3) (2011) 352–355.
[34] N. Beaumont, J.S. Castrucci, P. Sullivan, G.E. Morse, A.S. Paton, Z.H. Lu, T.P. Bender, T.S. Jones, J. Phys. Chem. C 118 (27) (2014) 14813–14823.
[35] S.E. Morris, M. Shtein, Org. Electron. 15 (12) (2014) 3795–3799.
[36] C.H. Peters, I.T. Sachs-Quintana, J.P. Kastrop, S. Beaupre, M. Leclerc, M.D. McGehee, Adv. Energy Mater. 1 (4) (2011) 491–494.
[37] M.O. Reese, A.J. Morfa, M.S. White, N. Kopidakis, S.E. Shaheen, G. Rumbles, D.S. Ginley, Sol. Energy Mater. Sol. Cells 92 (7) (2008) 746–752.
[38] I. Hancox, P. Sullivan, K.V. Chauhan, N. Beaumont, L.A. Rochford, R.A. Hatton, T.S. Jones, Org. Electron. 11 (12) (2010) 2019–2025.